Binding of Organometallic Ruthenium(II) and Osmium(II) Complexes to an Oligonucleotide: A Combined Mass Spectrometric and Theoretical Study†

Antoine Dorcier, Paul J. Dyson,* Christian Gossens, Ursula Rothlisberger,* Rosario Scopelliti, and Ivano Tavernelli

Institut des Sciences et Ingénierie Chimiques, Ecole Polytechnique Fédérale de Lausanne (EPFL), CH-1015 Lausanne, Switzerland

Received December 10, 2004

A series of ruthenium(II) and osmium(II) *p*-cymene dichloride complexes with either a pta (1,3,5-triaza-7-phosphatricyclo[3.3.1.1]decane) or [pta-Me]Cl ligand which exhibit anticancer activity have been prepared and characterized by ^{1}H and ^{31}P NMR spectroscopy and mass spectrometry. Three of the complexes, viz. [Os(η^6-*p*-cymene)Cl_2(pta)] and [M(η^6-*p*-cymene)Cl_2(pta-Me)]Cl (M = Ru, Os), have also been characterized by single-crystal X-ray diffraction. The pta complexes are selective anticancer agents, whereas the pta-Me^+ complexes are indiscriminate and damage both cancer and healthy cells but represent models for the protonated pta adduct which has been implicated in drug activity. To establish a link between their biological activity and the effect they have on DNA (a likely in vivo target), the reactivity of the complexes toward a 14-mer oligonucleotide (5′-ATACATGGTACATA-3′) was studied using electrospray ionization mass spectrometry. It was found that the complexes bind to the oligonucleotide with loss of chloride and in some cases loss of the arene. Loss of arene appears to be most facile with the ruthenium−pta complexes but also takes place with the ruthenium−pta-Me complexes, whereas arene loss is not observed for the osmium complexes. In addition, as pH is reduced, increased binding to the oligonucleotide is observed, as evidenced from mass spectrometric relative intensities. Binding energies between the metal centers and the surrounding ligands were calculated using density functional theory (DFT). The calculated energies rationalize the experimentally observed tendencies for arene loss and show that the pta ligands are relatively strongly bound. Exchange of metal center (ruthenium versus osmium), methylation or protonation of the pta ligand, or change of the arene (*p*-cymene versus benzene) results in significant differences in the metal−arene binding energies while leaving the metal−phosphine bond strength essentially unchanged. Significantly lower binding energies and reduced hapticity are predicted for the exchange of arene by nucleobases. The latter show higher binding energies for nitrogen σ-bonding than for π-bonding.

Introduction

Following the success of cisplatin in the clinic since its discovery in 1965,[1] which remains the most widely used anticancer drug, employed in the treatment of approximately 70% of all cancer patients, many inorganic and organometallic compounds have been evaluated as pharmaceuticals.[2] Although the mechanism by which such compounds exert their medicinal effect is very complicated and is still a matter of debate, DNA interactions are generally considered to be critical. Platinum compounds have been shown to bind to DNA in several modes, and the X-ray structure of cisplatin bound to duplex DNA reveals that intrastrand cross-linking is combined with a hydrogen-bonding interaction.[3] The field of organometallic anticancer compounds dates back to the pioneering work of Köpf and Köpf-Maier, who investigated the antitumor activity of early-transition-metal cyclopentadienyl (metallocene) complexes, in the late 1970s.[4] Although organometallic compounds have been evaluated most extensively as reagents to combat cancer, other medicinal applications have also been investigated, including parasitic, viral, microbial, and, most recently, cardioprotection using metal carbonyl complexes.[5] One compound, titanocene dichloride, has already completed phase II clinical trials,[6] and a second compound, ferrocifen, which is a ferrocenyl derivative of tamoxifen,[7] looks set to enter clinical trials soon.[8] Main-group organometallic compounds such as diorga-

* To whom correspondence should be addressed. E-mail: paul.dyson@epfl.ch (P.J.D.); ursula.roethlisberger@epfl.ch (U.R.).

† Dedicated to Richard (Dick) Fish on the occasion of his 65th birthday.

(1) Rosenberg, B.; Vancamp, L.; Krigas, T. *Nature* **1965**, *205*, 698.
(2) Clarke, M. J.; Zhu, F.; Frasca, D. R. *Chem. Rev.* **1999**, *99*, 2511. Wong, E.; Giandomenico, C. M. *Chem. Rev.* **1999**, *99*, 2451.
(3) Takahara, P. M.; Frederick, C. A.; Lippard, S. J. *J. Am. Chem. Soc.* **1996**, *118*, 12309.
(4) Koepf, H.; Koepf-Maier, P. *Angew. Chem.* **1979**, *91*, 509.
(5) Johnson, T. R.; Mann, B. E.; Clark, J. E.; Foresti, R.; Green, C. J.; Motterlini, R. *Angew. Chem., Int. Ed.* **2003**, *42*, 3722.
(6) Kopf-Maier, P. *Anticancer Res.* **1999**, *19*, 493.
(7) Top, S.; El Kaloun, B.; Vessieres, A.; Leclercq, G.; Laios, I.; Ourevitch, M.; Deuschel, C.; McGlinchey, M. J.; Jaouen, G. *ChemBioChem* **2003**, *4*, 754.
(8) Jaouen, G. Personal communication.

10.1021/om049022a CCC: $30.25 © 2005 American Chemical Society
Publication on Web 03/23/2005

notin(IV) derivatives have been known to have antiproliferative activity on specific cancers for many years,[9] but they also tend to have high general toxicities, which limits their applicability in the clinic.

Much of the recent focus on organometallic pharmaceuticals has centered on the application of group 8 compounds as anticancer drugs. As mentioned above, ferrocene-based compounds such as ferrocifen represent excellent candidates for clinical trials. While tamoxifen blocks the estrogen hormone receptor site in hormone-dependent breast cancers, the additional role of the ferrocenyl unit in ferrocifen is not fully understood, although it is possible that the ferrocenyl moiety is oxidized to release iron(III), which subsequently generates oxygen radical species that exert a cytotoxic effect, possibly by reacting with DNA in proximity to the binding domain. However, following the entrance of ruthenium compounds (although not organometallics) into the clinic for the treatment of antimetastasis tumors, viz. [ImH][*trans*-$RuCl_4$(DMSO)Im] (NAMI-A)[10] and [ImH][*trans*-$RuCl_4Im_2$] (KP1019),[11] interest in this metal has increased. NAMI-A and KP1019 contain ruthenium(III) centers which are thought to undergo reduction in vivo to ruthenium(II), presumed to be the active anticancer species. Accordingly, it has been postulated that ruthenium(II) complexes might prove to be interesting drug candidates, and this oxidation state is stabilized by the presence of organic ligands.

Consequently, a number of ruthenium(II)−arene compounds have been evaluated as anticancer agents. For example, coordination of the known anticancer agent 1-β-hydroxyethyl-2-methyl-5-nitroimidazole (metronidazole) to the ruthenium(II)−benzene fragment afforded a compound with selective cytotoxicity superior to that of metronidazole itself.[12] Sheldrick reported some ruthenium(II)−arene compounds with alanine- and guanine-derived coligands,[13] and while their anticancer activity was not included in the report, they were found to be cytotoxic toward P388 leukemia cells.[14] Thus far, the most detailed study has been undertaken on ruthenium(II)−arene complexes with ethylenediamine coligands: viz., [Ru(η^6-arene)Cl(dien)]$^+$ (dien = ethylenediamine).[15,16] These complexes have been shown to exhibit selectivity toward N7 of guanine bases, and the reactivity of the various binding sites of nucleobases toward [Ru(η^6-biphenyl)Cl(dien)]$^+$ decreases in the order G(N7) > I(N7) > I(N1), T(N3) > C(N3) > A(N7), A(N1). The selectivity appears to be controlled by the ethylenediamine NH_2 groups, which H-bond with exocyclic oxygens but are nonbonding and repulsive toward the exocyclic amino groups of the nucleobases. It has also been proposed that hydrophobic interactions between the arene ligand and DNA could also facilitate DNA binding, and a direct correlation between cytotoxicity and the size of the arene was observed. A series of ruthenium(II)−arene compounds with disulfoxide ligands have been tested in vitro for anticancer activity. Although the interactions of the ruthenium(II)−arene compounds have been most extensively studied with DNA, Ru(η^6-C_6H_6)Cl_2(Me_2SO) has been shown to inhibit topoisomerase II.[17] The ethylenediamine compounds mentioned above were screened for activity as topoisomerase II inhibitors but were found to be inactive.

Our attention has focused on ruthenium(II)−arene complexes combined with the 1,3,5-triaza-7-phosphatricyclo[3.3.1.1]decane (pta) ligand.[18,19] The compound [Ru(η^6-*p*-cymene)Cl_2(pta)] was found to exhibit pH-dependent DNA damage such that at the pH typical of hypoxic cells DNA was damaged, whereas at the pH characteristic of healthy cells, little or no damage was detected. Such behavior was ascribed to the pta ligand which can be protonated at low pH, and the protonated form was considered to be the active agent. Subsequently, it has been observed that [Ru(η^6-*p*-cymene)Cl_2(pta)] exhibits highly selective anticancer activity in cell culture, destroying cancer cells while having almost no observable effect on healthy cells. In contrast, the model compound for the protonated derivative, [Ru(η^6-*p*-cymene)Cl_2(pta-Me)]$^+$, has an indistinguishable toxicity against both cancer and healthy cells.

To understand more fully the mode of action of the ruthenium(II)−arene pta complexes, we have conducted a detailed study of their binding (and that of osmium analogues) to an oligonucleotide, using a combined experimental−theoretical approach. Herein, we describe the outcome from these studies.

Results and Discussion

Ruthenium(II) and osmium(II) complexes of the type [M(η^6-*p*-cymene)Cl_2(L)] (L = pta, pta-Me$^+$; Chart 1) were prepared from the direct reaction of the dimer [M(η^6-*p*-cymene)(μ-Cl)Cl]$_2$ with 2 equiv of the appropriate phosphine, following essentially a literature protocol (compounds **1**,[18] **5**,[19] and **7**[15,16] are known). The pta ligand and its methyl derivative, pta-Me$^+$, are water-soluble, and the resulting complexes are also highly soluble in water.

All the new complexes have been characterized by ^{1}H and ^{31}P NMR spectroscopy and electrospray ionization mass spectrometry (ESI-MS). The ^{1}H NMR spectra of compounds **2**−**4** contain peaks between 4.2 and 5.1 ppm that correspond to the methylene protons attached to the pta or pta-Me$^+$ ligands; the methyl group protons

(9) Crowe, A. J.; Smith, P. J.; Atassi, G. *Chem.-Biol. Interact.* **1980**, *32*, 171. Crowe, A. J.; Smith, P. J.; Atassi, G. *Inorg. Chim. Acta* **1984**, *93*, 179.

(10) Sava, G.; Capozzi, I.; Bergamo, A.; Gagliardi, R.; Cocchietto, M.; Masiero, L.; Onisto, M.; Alessio, E.; Mestroni, G.; Garbisa, S. *Int. J. Cancer* **1996**, *68*, 60.

(11) Galanski, M.; Arion, V. B.; Jakupec, M. A.; Keppler, B. K. *Curr. Pharm. Design* **2003**, *9*, 2078.

(12) Dale, L. D.; Tocher, J. H.; Dyson, T. M.; Edwards, D. I.; Tocher, D. A. *Anti-Cancer Drug Design* **1992**, *7*, 3.

(13) Sheldrick, W. S.; Heeb, S. *Inorg. Chim. Acta* **1990**, *168*, 93.

(14) Heeb, S. In Dissertation, Ruhr-Universität Bochum, 1990.

(15) Aird, R. E.; Cummings, J.; Ritchie, A. A.; Muir, M.; Morris, R. E.; Chen, H.; Sadler, P. J.; Jodrell, D. I. *Br. J. Cancer* **2002**, *86*, 1652. Chen, H.; Parkinson, J. A.; Morris, R. E.; Sadler, P. J. *J. Am. Chem. Soc.* **2003**, *125*, 173. Chen, H.; Parkinson, J. A.; Parsons, S.; Coxall, R. A.; Gould, R. O.; Sadler, P. J. *J. Am. Chem. Soc.* **2002**, *124*, 3064. Morris, R.; Habtemariam, A.; Guo, Z.; Parsons, S.; Sadler, P. J. *Inorg. Chim. Acta* **2002**, *339*, 551. Novakova, O.; Chen, H.; Vrana, O.; Rodger, A.; Sadler, P. J.; Brabec, V. *Biochemistry* **2003**, *42*, 11544. Wang, F.; Chen, H.; Parkinson, J. A.; Murdoch, P. d. S.; Sadler, P. J. *Inorg. Chem.* **2002**, *41*, 4509. Wang, F.; Chen, H.; Parsons, S.; Oswald, I. D. H.; Davidson, J. E.; Sadler, P. J. *Chem. Eur. J.* **2003**, *9*, 5810.

(16) Morris, R. E.; Aird, R. E.; Murdoch, P. d. S.; Chen, H.; Cummings, J.; Hughes, N. D.; Parsons, S.; Parkin, A.; Boyd, G.; Jodrell, D. I.; Sadler, P. J. *J. Med. Chem.* **2001**, *44*, 3616.

(17) Gopal, Y. N. V.; Jayaraju, D.; Kondapi, A. K. *Biochemistry* **1999**, *38*, 4382.

(18) Allardyce, C. S.; Dyson, P. J.; Ellis, D. J.; Heath, S. L. *Chem. Commun.* **2001**, 1396.

(19) Allardyce, C. S.; Dyson, P. J.; Ellis, D. J.; Salter, P. A.; Scopelliti, R. *J. Organomet. Chem.* **2003**, *668*, 35.

Chart 1

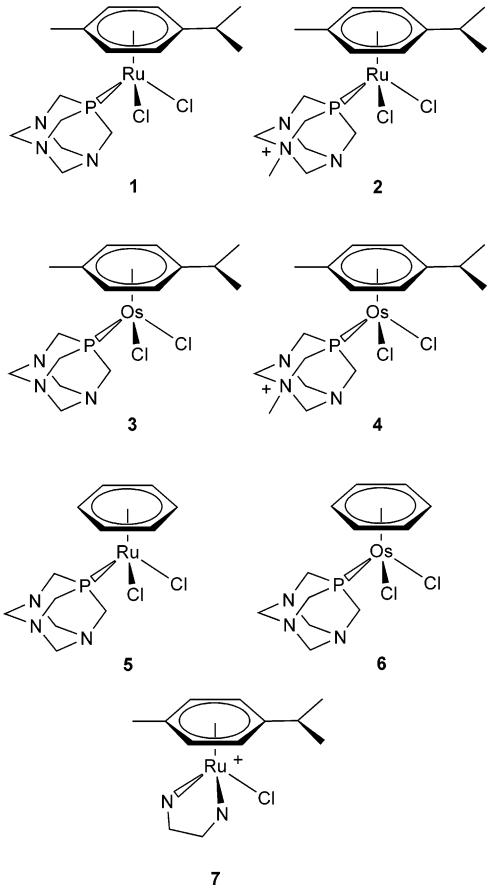

on the pta-Me$^+$ ligand are observed at 2.84 ppm for both **2** and **4**. The arene ligand protons are observed between 5.7 and 6.0 ppm, with the $-CH(CH_3)_2$ proton in the *p*-cymene species displaying a characteristic septet at ca. 2.65 ppm. The methyl group protons on the *p*-cymene moiety in **2**−**4** lie in the range 2.0−2.2 ppm. The ^{31}P NMR spectra are very simple, exhibiting a singlet resonance at −22.4 ppm for **2** and at −80.4 and −63.7 ppm for the osmium complexes **3** and **4**, respectively. The ESI mass spectra of the pta complexes exhibit peaks corresponding to loss of chloride, viz. [M(arene)Cl(pta)]$^+$, whereas the pta-Me$^+$-based complexes, which are naturally charged, exhibit intact parent ion peaks.

The solid-state structures of [Ru(η^6-*p*-cymene)Cl$_2$(pta-Me)]Cl (**2**), [Os(η^6-*p*-cymene)Cl$_2$(pta)] (**3**), and [Os(η^6-*p*-cymene)Cl$_2$(pta-Me)]Cl (**4**) have been determined by single-crystal X-ray diffraction on crystals grown from deuterated chloroform for **3** and by slow diffusion of pentane into a methanol solution of **2** or **4**. The molecular structures of **2**−**4** are illustrated in Figures 1−3, respectively, and key bond parameters are given in the captions. Crystal data and details of the structure determinations are listed in Table 1.

The molecular structures of **2**−**4** display the characteristic "piano stool" geometry and bond distances and angles very similar to those observed in related compounds.[20] The aromatic ring is tilted toward the MCl$_2$ moiety (where M = Ru, Os), whereas the vector connecting the metal and the phosphorus centers bisects the *p*-cymene in a perpendicular manner with respect to its substituents, presumably due to steric hindrance. All the angles involving the "legs" of the "piano stool"

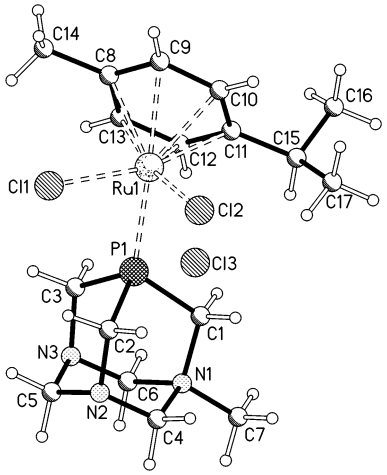

Figure 1. Molecular structure of **2** in the solid state. Key bond lengths (Å) and angles (deg): Ru1−Cl1, 2.3903(11); Ru1−Cl2, 2.4101(11); Ru1−P1, 2.2753(11); P1−Ru1−Cl2, 84.53(4); P1−Ru1−Cl1, 80.30(4); Cl2−Ru1−Cl1, 87.39(4), Ru1−η^6, 1.692(2).

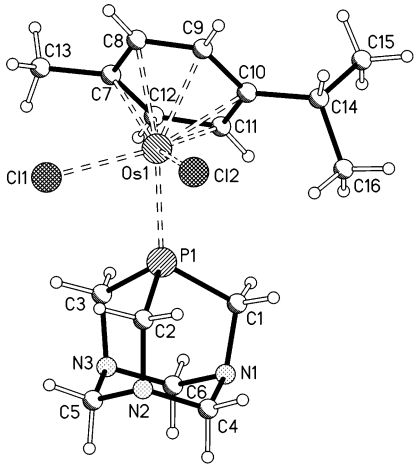

Figure 2. Molecular structure of **3** in the solid state. Key bond lengths (Å) and angles (deg): Os1−Cl1, 2.4344(15); Os1−Cl2, 2.4194(15); Os1−P1, 2.3324(16); P1−Os1−Cl2, 86.75(5); P1−Os1−Cl1, 81.61(6); Cl2−Os1−Cl1, 86.27(5), Os1−η^6, 1.698(3).

structures are less than 90°. The Os−Cl bond distances are very similar (varying from 2.4194(15) to 2.437(4) Å) and, as expected, longer than the Ru−Cl lengths (average value 2.400(1) Å). The same feature is observed for the Os−P bond lengths (Os1−P1 = 2.3324(16) Å for **3** and 2.319(4) Å for **4**) with respect to the Ru−P bond distance (2.2753(11) Å). All crystal structures discussed here show a large number of weak hydrogen bonds between C−H hydrogen atoms and the Cl or N centers.

Single-Stranded-Oligomer Binding Studies. All of the compounds are active anticancer agents, as demonstrated in cell culture using the model employed to evaluate NAMI-A.[21] The pta species are selective

(20) Arena, C. G.; Calamia, S.; Faraone, F.; Graiff, C.; Tiripicchio, A. *Dalton* **2000**, 3149. Bell, A. G.; Kozminski, W.; Linden, A.; von Philipsborn, W. *Organometallics* **1996**, *15*, 3124. Bhalla, R.; Boxwell, C. J.; Duckett, S. B.; Dyson, P. J.; Humphrey, D. G.; Steed, J. W.; Suman, P. *Organometallics* **2002**, *21*, 924. Durran, S. E.; Smith, M. B.; Slawin, A. M. Z.; Steed, J. W. *Dalton* **2000**, 2771. Faller, J. W.; Parr, J. *Organometallics* **2000**, *19*, 3556. Parr, J.; Smith, M. B.; Elsegood, M. R. J. *J. Organomet. Chem.* **2002**, *664*, 85. Thoumazet, C.; Melaimi, M.; Ricard, L.; Mathey, F.; Le Floch, P. *Organometallics* **2003**, *22*, 1580.

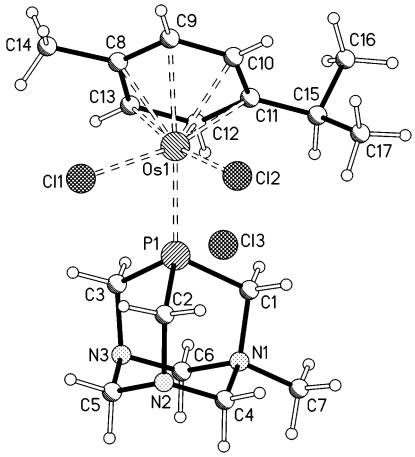

Figure 3. Molecular structure of **4** in the solid state. Key bond lengths (Å) and angles (deg): Os1−Cl1, 2.436(4); Os1−Cl2, 2.436(4); Os1−P1, 2.318(4); P1−Os1−Cl2, 84.89(14); P1−Os1−Cl1, 80.50(14); Cl2−Os1−Cl1, 85.99(14), Os1−η^6, 1.712(7).

toward cancer cells, with almost no effect observed on healthy cells. In contrast, the pta-Me$^+$ compounds **2** and **4** are equally toxic toward cancer cells and healthy cells. The traditional target for metal-based anticancer drugs is DNA; ruthenium compounds are known to induce apoptosis via the mitochondria, and damage of mitrochondrial DNA is implicated in the activity of several important metal-based anticancer drugs.[22] Accordingly, we decided to study the reactivity of compounds **1**−**4** with an oligonucleotide DNA model, to determine whether the differences in selectivity between the pta and pta-Me$^+$ compounds could be delineated. The single-stranded 14-mer 5′-ATACATGGTACATA-3′ was selected for the study, since it has been previously used for an in-depth study on **7** and related compounds in which the *p*-cymene has been replaced by other arenes.[16] Essentially, the technique involves incubation of the organometallic compound with the oligonucleotide followed by analysis by electrospray ionization mass spectrometry (ESI-MS). Samples were prepared according to three different stoichiometries, viz. 14-mer to complex ratios of 1:1, 1:2, and 1:5, and were incubated in water for 72 h at 37 °C. Following incubation the solutions were desalted using a C18 HPLC column and injected directly into the mass spectrometer (no separation of the different adducts was carried out). The negative ion ESI deconvolution mass spectra for the 1:1 incubation with [Ru(η^6-*p*-cymene)Cl$_2$(pta)] (**1**) and 1:1 incubation with [Os(*p*-cymene)Cl$_2$(pta)] (**3**) are shown in Figures 4 and 5 as illustrative examples.

The results obtained from these experiments are summarized in Table 2, and close inspection of these data reveals a number of trends. Under the conditions employed, all the compounds are able to bind to the oligomer (as mentioned above, this has already been demonstrated for **7**). The ruthenium complexes **1** and **2** coordinate to the oligomer with loss of chloride and with loss of the arene, although loss of the arene depends to some extent on the ratio of oligomer to complex: i.e., as the amount of complex is increased, only partial loss of the arene is observed. The pta and pta-Me$^+$ ligands in **1**−**4** are always present, suggesting that they remain coordinated to the ruthenium or osmium centers following binding. In aqueous solution the chloride ligands are rapidly lost from **1**−**7**, although it is highly dependent on the concentration of chloride in solution. However, from the mass spectrometric data it is not unreasonable to assume that binding of the complexes takes place initially via chloride (or water) substitution, and subsequently, loss of the arene takes place. Loss of the arene is not observed for the osmium complexes **3** and **4** and complex **7**. It would also appear that loss of the arene is less favored for the pta-Me$^+$ complexes relative to the pta compounds. However, under the conditions employed, the pta-Me$^+$ complexes appear to be more reactive than the pta complexes, presumably due to the higher affinity of the more highly charged species with a polyanion.

Thus far, it has not been possible to unequivocally establish a preferential site of complexation for **1**−**4** on the 14-mer, and considering that a large number of adducts are produced in the reaction of the 14-mer with 5 equiv of the complex, it is probable that highly specific binding to single-stranded DNA does not take place. In addition, at lower pH the pta complexes show increased levels of binding to the oligomer relative to normal pH (based on relative intensities), which is in keeping with the hypothesis that the pta compounds are more active at low pH.

Computational Rationalization. Density functional theory (DFT) calculations are a well-established tool to describe the geometry and binding energies in transition-metal complexes and are frequently used to rationalize mass spectrometric experiments.[23,24] Very little experimental thermochemical data on organoruthenium complexes are available, and the existing literature has a focus primarily on cyclopentadienyl derivatives.[25] Using DFT the relative binding energies for the arene and pta ligands in complexes **1**−**7** have been investigated in order to elucidate the experimental observation of arene loss on binding of compounds **1** and **2** with single-stranded DNA. The compounds investigated differ in the type of metal (ruthenium or osmium), the pta ligand (pta, N-methylated pta, or N-protonated pta) and the arene system (*p*-cymene or benzene). The related monofunctional compound **7** containing a chelating diamine ligand has been investigated for comparison purposes.

The chloride species shown in Chart 1 have been used as model compounds for the computational study, although they undergo hydrolysis prior to DNA binding. Compounds **2** and **4** are used experimentally as pH-independent model compounds for the N-protonated derivatives (**1-H**$^+$ and **3-H**$^+$) of compounds **1** and **3**. The calculations on the charged species were performed in

(21) Mosmann, T. *J. Immunol. Methods* **1983**, *65*, 55.
(22) Olivero, O. A.; Semino, C.; Kassim, A.; Lopezlarraza, D. M.; Poirier, M. C. *Mutation Res.* **1995**, *346*, 221.
(23) Adlhart, C.; Hinderling, C.; Baumann, H.; Chen, P. *J. Am. Chem. Soc.* **2000**, *122*, 8204. Aebischer, N.; Sidorenkova, E.; Ravera, M.; Laurenczy, G.; Osella, D.; Weber, J.; Merbach, A. E. *Inorg. Chem.* **1997**, *36*, 6009. Dolker, N.; Frenking, G. *J. Organomet. Chem.* **2001**, *617*−*618*, 225. McGrady, J. E.; Dyson, P. J. *J. Organomet. Chem.* **2000**, *607*, 203. Stoyanov, S. R.; Villegas, J. M.; Rillema, D. P. *Inorg. Chem.* **2002**, *41*, 2941. Vrkic, A. K.; Taverner, T.; James, P. F.; O'Hair, R. A. J. *Dalton* **2004**, 197.
(24) Tamm, M.; Dressel, B.; Lugger, T.; Frohlich, R.; Grimme, S. *Eur. J. Inorg. Chem.* **2003**, 1088.
(25) Nolan, S. P. *Comments Inorg. Chem.* **1995**, *17*, 131. Turnbull, A. G. *Aust. J. Chem.* **1967**, *20*, 2757.

Table 1. Crystal Data and Details of the Structure Determination for 2−4

	2	3	4
chem formula	$C_{17.5}H_{31}Cl_3N_3O_{0.5}PRu$	$C_{18}H_{28}Cl_8N_3OsP$	$C_{17.5}H_{31}Cl_3N_3O_{0.5}OsP$
formula wt	529.84	791.20	618.97
cryst syst	monoclinic	monoclinic	monoclinic
space group	$P2_1/c$	$P2_1/n$	$P2_1/c$
a (Å)	13.4320(13)	10.579(2)	13.5918(20)
b (Å)	10.5988(10)	12.7402(9)	10.7345(9)
c (Å)	16.2393(15)	20.977(4)	16.442(2)
β (deg)	113.411(9)	101.171(16)	113.142(14)
V (Å^3)	2121.6(3)	2773.7(8)	2205.9(5)
Z	4	4	4
D_{calcd} (g cm^{-3})	1.659	1.895	1.864
F(000)	1084	1536	1212
μ (mm^{-1})	1.203	5.439	6.227
temp (K)	140(2)	140(2)	140(2)
wavelength (Å)	0.710 73	0.710 70	0.710 73
no. of measd rflns	12048	16359	12057
no. of unique rflns	3373	4836	3764
no. of unique rflns ($I > 2\sigma(I)$)	2819	4353	3220
no. of data/params	3373/239	4836/281	3764/244
R1[a] ($I > 2\sigma(I)$)	0.0426	0.0426	0.0774
wR2[a] (all data)	0.1147	0.1139	0.1700
GOF[b]	1.022	1.128	1.196

[a] $R1 = \sum||F_o| - |F_c||/\sum|F_o|$; $wR2 = \{\sum[w(F_o^2 - F_c^2)^2]/\sum[w(F_o^2)^2]\}^{1/2}$. [b] $GOF = \{\sum[w(F_o^2 - F_c^2)^2]/(n - p)\}^{1/2}$, where n is the number of data and p is the number of parameters refined.

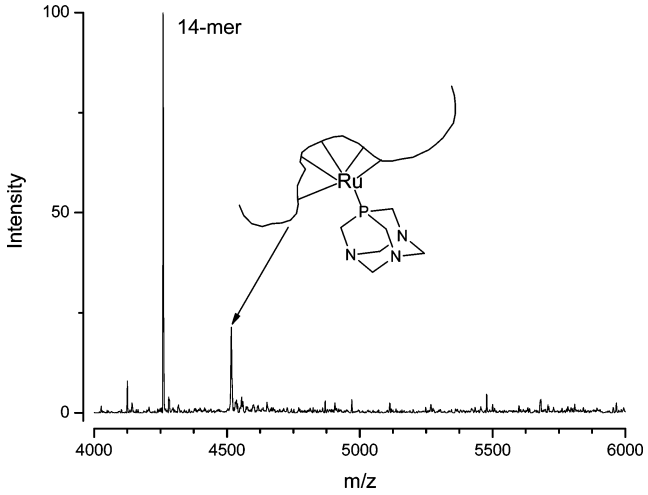

Figure 4. Negative ion ESI mass spectrum (deconvoluted) of 14-mer + **1** (1:1) in water (72 h, 37 °C).

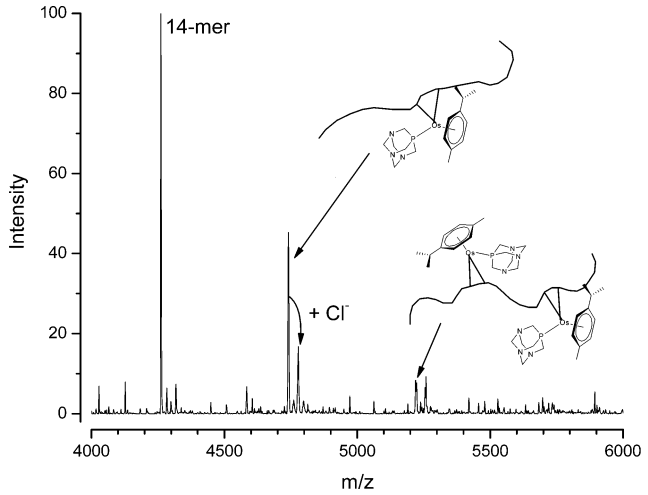

Figure 5. Negative ion ESI mass spectrum (deconvoluted) of 14-mer + **3** (1:1) in water (72 h, 37 °C).

the absence of counterions. Moreover, the benzene derivatives **5** and **6** were included to investigate the influence of a modified arene on the ligand binding energies. It was found that the calculated binding energies for the metal−arene interaction change substantially upon modifications in the compound (viz. nature of the arene, protonation or methylation of the pta, and the metal type), whereas the metal−phosphine bond is only slightly affected.

(a) Arene Binding. All osmium compounds show a significantly higher arene binding energy (BE) than their ruthenium analogues, a tendency that has been calorimetrically observed also for the metallocenes, $M(C_5H_5)_2$, where M = Fe, Ru, Os.[26] As shown in Table 3, the pairs **5/6**, **1/3**, **2/4**, and **1-H**$^+$/**3-H**$^+$ with BEs of 19.5/23.5, 21.2/24.8, 31.7/33.4, and 32.0/33.6 kcal/mol, respectively, exhibit systematic stronger binding interaction in the case of the osmium compounds. The *p*-cymene ligand in the couples **1/5** and **3/6** has a stronger bond to the same metal than does the benzene ligand. However, this effect is less pronounced than that of the central metal. The N-protonated compounds **1-H**$^+$ and **3-H**$^+$ show the same metal−arene binding energy as their N-methylated analogues. In our gas-phase calculations the metal−arene binding energies for the positively charged compounds **2**, **1-H**$^+$, **4**, and **3-H**$^+$ are significantly higher than for their neutral analogues. This trend of increased metal−arene bond strength with higher positive charge is even stronger for the positively charged (in vacuo) aqua complexes of compounds **1** and **7** (Table S7). As the calculations are carried out in the absence of a solvent, the polarizable arene stabilizes the positive charge. It is, however, doubtful if this large difference in binding energy between the neutral and charged compounds accurately represents the reactive properties of these compounds in solution. For reasons of consistency, the calculated increase of metal−arene binding energies in the order **5** < **1** < **6** < **3** ≪ **2** ≈ **1-H**$^+$ < **4** ≈ **3-H**$^+$ ≪ **7** allows only for comparison among neutral or among charged compounds. The *p*-cymene compound **7** shows by far the strongest ruthenium−arene binding energy. Therefore, the computational results rationalize the experimental data very nicely.

(26) Fischer, E. O.; Grubert, H. *Chem. Ber.* **1959**, *92*, 2301.

Table 2. Species Observed after Deconvolution of the ESI Spectra from the Incubations of 1−4 and 7 with the 14-mer 5′-ATACATGGTACATA-3′ at Various 14-mer to Complex Ratios[a]

	1:1	1:2
1	14-mer [14-mer + Ru(pta)] (20%)	[14-mer + Ru(pta)] 14-mer (45%) [14-mer + Ru(pta) + Ru(η^6-*p*-cymene)(pta)] (18%)
2	14-mer [14-mer + Ru(pta-Me)] (17%) [14-mer + 2 Ru(pta-Me)] (10%) [14-mer + Ru(pta-Me) + Ru(η^6−*p*-cymene)(pta-Me)] (5%)	[14-mer + Ru(pta-Me)] 14-mer (95%) [14-mer + Ru(η^6-*p*-cymene)(pta-Me)Cl] (45%) [14-mer + Ru(η^6-*p*-cymene)(pta-Me)] (30%)
3	14-mer [14-mer + Os(η^6-*p*-cymene)(pta)] (47%) [14-mer + Os(η^6-*p*-cymene)(pta)Cl] (18%) [14-mer + Os(η^6-*p*-cymene)(pta) + Os(η^6−*p*-cymene)(pta)Cl] (9%) [14-mer + 2 Os(η^6-*p*-cymene)(pta)] (8%)	14-mer [14-mer + Os(η^6-*p*-cymene)(pta)] (70%) [14-mer + Os(η^6-*p*-cymene)(pta)Cl] (27%) [14-mer + 2 Os(η^6-*p*-cymene)(pta)] (25%) [14-mer + Os(η^6-*p*-cymene)(pta) + Os(η^6−*p*-cymene)(pta)Cl] (20%)
4	14-mer [14-mer + Os(η^6-*p*-cymene)(pta-Me)] (65%) [14-mer + Os(η^6-*p*-cymene)(pta-Me)Cl] (8%) [14-mer + Os(η^6-*p*-cymene)(pta-Me) + Os(η^6−*p*-cymene)(pta-Me)Cl] (8%)	[14-mer + Os(η^6-*p*-cymene)(pta-Me)] 14-mer (67%) [14-mer + 2 Os(η^6-*p*-cymene)(pta-Me)] (28%) [14-mer + Os(η^6-*p*-cymene)(pta-Me)Cl] (10%) [14-mer + Os(η^6-p-cymene)(pta-Me) + Os(η^6−*p*-cymene)(pta-Me)Cl] (8%)
7	[14-mer + Ru(η^6-*p*-cymene)(en)] 14-mer (98%) [14-mer + 2 Ru(η^6-*p*-cymene)(en)] (25%)	[14-mer + Ru(η^6-*p*-cymene)(en)] [14-mer + 2 Ru(η^6-*p*-cymene)(en)] (60%) 14-mer (40%)

[a] Mass of the 14-mer strand, *m/z* 4261. The percentage in parentheses corresponds to the relative intensity (first species at 100%).

Table 3. Calculated Metal−Arene Binding Energies[a] in kcal/mol

	compd								
	5	**1**	**6**	**3**	**2**	**1-H$^+$**	**4**	**3-H$^+$**	**7**
energy	19.5	21.2	23.5	24.8	31.7	32.0	33.4	33.6	55.5
relative to **5**	0.0	1.7	4.0	5.3	12.2	12.5	13.9	14.1	36.0

[a] B3LYP/basis 3 (BSSE corrected).

Table 4. Calculated Metal−pta/dien Binding Energies[a] in kcal/mol

	compd								
	5	**1**	**6**	**3**	**2**	**1-H$^+$**	**4**	**3-H$^+$**	**7**
energy	19.8	18.6	19.3	18.2	17.9	18.4	17.1	17.5	63.7
relative to **5**	0	−1.2	−0.5	−1.6	−1.9	−1.4	−2.7	−2.3	43.9

[a] B3LYP/basis 3 (BSSE corrected).

(b) pta Binding. In contrast to the observed trends in metal−arene interaction energies, the metal−pta binding energy does not show significant changes among the investigated compounds **1**−**6** (see Table 4). In the binding experiments, the pta ligand is always present in DNA adducts, regardless of the nature of the metal or the arene. The osmium−pta BEs are slightly weaker (ca. 0.5−1.0 kcal/mol) than those of their ruthenium analogues. The *p*-cymene compounds **1** and **3** show a slightly less stable metal−pta bond than the benzene analogues **5** and **6**. In contrast to the metal−arene interactions, the metal−pta binding energy turns out to be nearly independent of a positive charge on the pta ligand. In fact, only a slightly lower metal−pta binding energy was calculated for compounds that carry a positive charge. Among these compounds the N-protonated species of compounds **1** and **3** have a slightly stronger metal−pta bond than the N-methylated analogues **2** and **4**. As this difference is only on the order of 0.5 kcal/mol, the latter appears to be a good pH-independent model for the former. Not surprisingly, the chelating *N,N*-ethylenediamine (dien) ligand in compound **7** was calculated to be much more strongly bound than the monodentate pta ligand in compounds **1**−**6**.

(c) Comparison between Arene and pta Binding Energies. Among the pta-containing compounds, the ruthenium−arene interactions are calculated to be stronger than the ruthenium−phosphine bonds, which conflicts with the oligomer binding studies described above. The different natures of these bonds, however, calls into question a direct comparison of the binding energies of these two ligand coordination types. Although the calculated binding energies suggest that the pta ligand leaves first, they do not exclude the experimentally observed loss of arene, which might be controlled by the kinetics and the influence of environment. We observed that within the Kohn−Sham formalism and a frozen orbital approximation the HOMO energy is nearly independent of the metal. The LUMO energies, however, were calculated to be 0.4 eV higher for the osmium compounds than for their ruthenium analogues, making them more susceptible to nucleophilic attack. It is worth noting that loss of the arene is frequently observed when related compounds are employed in catalytic applications.[27] Moreover, a loss of the η^6 arene in pseudo-octahedral compounds opens three new ligand positions, whereas a leaving pta can only be replaced by one ligand. The total binding energy of three σ-bound ligands might compensate for the arene−ruthenium binding energy. In test calculations on different spin states a lowering of hapticity from η^6 to a minimum of η^2 was observed for the triplet of compound **5** but not for compound **7** (Table S5a-b; Supporting Information). This result, together with the observation that the energy difference between the singlet and triplet states is larger for **7** than for **5**, indicates that the arene in the pta-containing compounds is less strongly bound.

The N-methylated pta species **2** and **4** show the same ligand binding energies as the N-protonated pta species. As has been shown in a previous publication, the binding of **1** to DNA is pH dependent.[18] The strikingly

(27) Fuerstner, A.; Mueller, T. *J. Am. Chem. Soc.* **1999**, *121*, 7814. Hafner, A.; Muhlebach, A.; Van Der Schaaf, P. A. *Angew. Chem., Int. Ed.* **1997**, *36*, 2121.

Table 5. Selected Experimental (X-ray)/Calculated[a] Angles (deg) and Distances (Å) for 1−4

	M−Cl1	M−Cl2	M−P	P−M−Cl2	P−M−Cl1	Cl2−M−Cl1	M−η^6 [b]
1	2.41/2.44	2.43/2.44	2.30/2.33	83.4/82.3	87.1/89.9	87.2/83.8	1.69/1.76
2	2.39/2.43	2.41/2.45	2.28/2.31	84.5/83.0	80.3/80.4	87.4/89.3	1.69/1.77
3	2.43/2.47	2.42/2.47	2.33/2.35	86.8/84.3	81.6/82.1	86.3/87.9	1.70/1.74
4	2.44/2.45	2.44/2.47	2.32/2.32	84.9/83.9	80.5/80.8	86.0/87.1	1.71/1.76

[a] B3LYP/basis 3. [b] Distance between the metal and the center of the aromatic ring.

similar binding energies of these two series of compounds are a further validation for the choice of the N-methylated pta species as a pH-independent model for the N-protonated pta species.

(d) Arene Exchange with DNA Bases: A potential replacement for a lost η^6 arene ring in the pta-containing ruthenium compounds are the heterocyclic, aromatic nucleobases guanine, adenine, thymine, and cytosine. However, whereas arene exchange is known to occur,[28] only a few nitrogen-, phosphorus-, sulfur-, and boron-containing π-bonded heterocycles have been reported in transition-metal complexes and aromatic rings containing two heteroatoms are even more rare in this context.[29] The replacement of a CH unit in benzene with a nitrogen or NH unit opens the possibility of the aromatic heterocycles binding to a transition metal via either a σ or a π bond.

When the arene in compound **5** is exchanged for a π-bound nucleobase, substantial structural changes in form of a puckering of the aromatic ring system are observed, except for adenine.

Both pyrimidine bases, cytosine and thymine, were found to bind to the ruthenium center via their N1, C6, and C5 atoms. Starting from different arene analogue structures the formation of a η^3-π complex was the only resulting stable geometry.

The purines, adenine and guanine, offer (in principle) two heterocyclic aromatic rings that could form a π complex with the ruthenium center. However, binding to the ruthenium via the five-membered ring does not appear to correspond to a local energy minimum. With the arene analogue structures as starting point, the formation of σ complexes is exclusively observed, via the N7 atom of purine. In the case of adenine the resulting complex is further stabilized via a H-bond between an amine hydrogen and a chloride. Binding to ruthenium via the six-membered ring of the purines yielded, in the case of adenine, a σ complex via the N3 atom. A more detailed analysis proved the existence of a local minimum in which the six-membered rings of adenine and guanine are π coordinated to ruthenium via their N1, C2, and N3 atoms and, in the case of adenine, also via C4.

The energy-minimized π-bonded products (Table 7, Figures 6 and 7) show a significantly lower binding energy for the pyrimidine and purine compounds than for the arene analogues (Table 6). Taking into account the observation that the observed π complexes of the purines are all less stable than the corresponding σ complexes, the latter should be the dominant products upon loss of arene. The observed σ complexes of the nucleobases (Table 8) are coordinationally unsaturated, and the addition of two further ligands might amount to a total gain in energy that makes the loss of arene energetically favorable.

Table 6. Calculated Metal−Arene/Nucleobase Binding Energies[a] in kcal/mol

−$RuCl_2$pta	π complex	σ complex
benzene	33.1	n.a.
p-cymene	37.4	n.a.
adenine 5-ring	no minimum obsd	22.9 (N7, NH_2−Cl)
adenine 6-ring	18.3 (η^{3-4}; N1, C2, N3, *C4*)	29.4 (N3, N9H−Cl)
guanine 5-ring	no minimum obsd	22.3 (N7)
guanine 6-ring	8.8 (η^3; N1, C2, N3)	18.0 (N3, NH_2−Cl1, N9H−Cl2)[b]
cytosine	18.6 (η^3; N1, C6, C5)	36.3 (N3, NH_2−Cl)[b]
thymine	14.2 (η^3 ; N1, C6, C5)	n.a.

[a] ADF2004, BP86/TZP/Zora. [b] Starting from a σ-bonded structure.

Table 7. Calculated Ruthenium−Ligand π Bond Lengths (Å) of Nucleobase−$RuCl_2$pta Compounds[a]

base-$RuCl_2$pta	P	N1	N3	C2	C4	C5	C6
adenine 6-ring	2.24	2.36	2.28	2.07	2.40	2.58	2.56
guanine 6-ring	2.22	2.27	2.26	2.08	2.60	3.03	3.06
cytosine	2.29	2.21	3.37	3.15	2.96	2.35	2.09
thymine	2.29	2.27	3.36	3.15	3.09	2.39	2.11

[a] ADF2004, BP86/TZP/Zora.

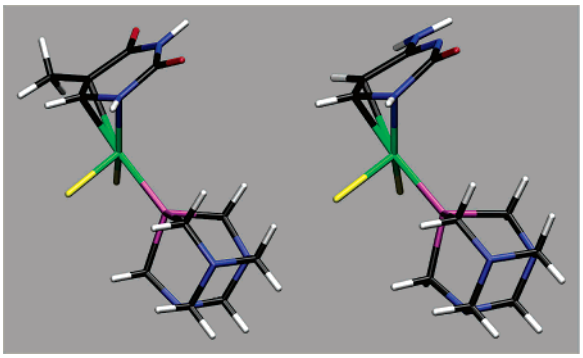

Figure 6. Optimized π-bound products of $RuCl_2$pta with thymine (left) and cytosine (right): Ru, green; C, black; H, white; Cl, yellow; P, purple; N, blue, O, red.

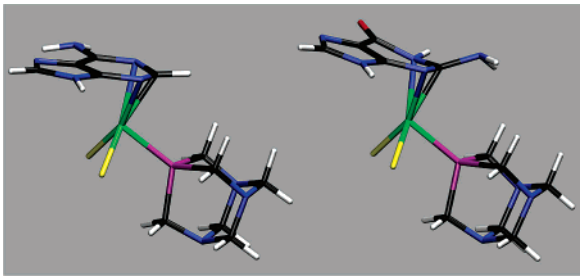

Figure 7. Optimized π-bound products of $RuCl_2$pta with adenine (left) and guanine (right).

(28) Tobita, H.; Hasegawa, K.; Minglana, J. J. G.; Luh, L.-S.; Okazaki, M.; Ogino, H. *Organometallics* **1999**, *18*, 2058.

(29) Bennett, M. A.; Neumann, H.; Thomas, M.; Wang, X. Q.; Pertici, P.; Salvadori, P.; Vitulli, G. *Organometallics* **1991**, *10*, 3237. Fish, R. H.; Fong, R. H.; Anh, T.; Baralt, E. *Organometallics* **1991**, *10*, 1209. Herberich, G. E.; Englert, U.; Pubanz, D. *J. Organomet. Chem.* **1993**, *459*, 1. Muetterties, E. L.; Bleeke, J. R.; Wucherer, E. J.; Albright, T. *Chem. Rev.* **1982**, *82*, 499. Pan, J.; Kampf, J. W.; Ashe, A. J., III. *Organometallics* **2004**, *23*, 5626. Wucherer, E. J.; Muetterties, E. L. *Organometallics* **1987**, *6*, 1691.

Table 8. Selected Calculated[a] Angles (deg) and Distances (Å) for σ Complexes of the $RuCl_2$pta Fragment with Nucleobases

base−$RuCl_2$pta	Ru−P	Ru−N	N−Ru−P	N−Ru−O[b]
adenine N7	2.18	2.08	101.9	177.2
adenine N3	2.17	2.12	99.3	170.0
guanine N7	2.19	2.09	103.6	163.2
guanine N3	2.18	2.09	105.5	172.2
cytosine N3	2.19	2.06	107.2	151.7

[a] ADF2004, BP86/TZP/Zora. [b] O is the center of the nucleobase ring.

Comparisons and Implications. The aqueous chemistry of transition-metal−arene compounds has been studied in some detail,[30] with the reaction of such compounds with nucleobases, nucleosides, and nucleotides being of particular focus.[31] These latter papers indicated that under physiological conditions such compounds could be of therapeutic use, but with the exception of the metallocenes, no biological data has been forthcoming. In the past few years, however, the anticancer properties of a series of ruthenium−arene complexes have emerged,[15,16,18,19] including some also with pta ligands closely related to those described herein, viz. Ru(η^5-arene)Cl(pta)$_2$ (arene = C_5H_5, C_5Me_5),[32] which has rekindled interest in the fundamental interactions of these compounds with DNA/RNA systems outlined in the earlier studies.

It is noteworthy for the ruthenium compounds described herein that in comparison to those reported by Sadler (compound **7** and its analogues), loss of the arene is observed, which could represent a new π-binding mechanism for a metal−DNA adduct. However, calculations indicate that such bonding is unlikely. It is much more likely that the single-stranded oligomer is sufficiently flexible to wrap around the metal center with the formation of multiple coordinative N-donor bonds. To bring about coordinative saturation of the ruthenium center, an interaction with phosphate may also be involved, in keeping with previous observations.[33] However, such a result could also implicate RNA's as the biological target, but at this stage, it is probably unwise to speculate any further in this direction. In comparison to cisplatin the bindings of the ruthenium and osmium compounds reported herein are nonspecific in their binding to the oligomer. However, it is worth noting that, unlike cisplatin, these compounds appear to be more specific in their cyctotoxicity toward cancer cells relative to healthy cells. Such data might suggest that a different DNA (or possibly RNA) binding mode is in operation, as suggested above, or perhaps that the actual target is different, such as a protein, although activation at low pH would appear to be the most critical factor. Closely related compounds have already been shown to inhibit proteins such as topoisomerases,[17] and we are currently trying to identify specific binding with these and other proteins of relevance, which will be the subject of a future report.

Experimental Section

[M(η^6-*p*-cymene)Cl_2]$_2$ (M = Ru,[34] Os[35]), [Ru(η^6-*p*-cymene)Cl_2(pta)],[18] [Ru(η^6-*p*-cymene))Ru(en)Cl]PF_6 (en = ethylenediamine),[15,16] and pta and [pta-Me]Cl[36] were prepared according to literature methods. All other reagents were obtained from commercial suppliers and used as received. NMR spectra were recorded on a Bruker Avance DPX 400 MHz spectrometer. ESI-MS of the complexes were obtained on a Thermofinigan LCQ Deca XP Plus quadrupole ion trap instrument set in positive mode (solvent, methanol; flow rate, 5 μL/min; spray voltage, 5 kV; capillary temperature, 100 °C; capillary voltage, 20 V), as described previously.[37]

Synthesis of [Ru(η^6-*p*-cymene)Cl_2pta-Me]Cl (2). A mixture of [Ru(η^6-*p*-cymene)Cl_2]$_2$ (100 mg, 0.163 mmol) and [pta-Me]Cl (67.8 mg, 0.326 mmol) was refluxed under nitrogen in MeOH (25 mL) for 4 h. After evaporation of the solvent under vacuum the residue was washed with ether (2 × 5 mL) and recrystallized from hot methanol. The product was obtained as orange crystals; yield 123.8 mg, 74%. ^{1}H NMR (MeOD-d_4, 400 MHz): δ 1.23 (d, 7 Hz, ArCH(CH_3)$_2$), 2.05 (s, ArCH_3), 2.70 (heptet, 7 Hz, ArCH(CH$_3$)$_2$), 2.84 (d, 2 Hz, N$^+$CH$_3$), 4.23 and 4.46 (d, 16 and 14.5 Hz, PCH_AH_BN), 4.61 and 4.67 (d, 13.5 Hz, NCH_AH_BN), 4.58 (d, 1 Hz, PCH_AH_BN$^+$), 4.97 and 5.10 (d, 12 Hz, PCH_AH_BN$^+$). ^{31}P NMR (MeOD-d_4, 162 Hz): δ −63.7. ESI-MS: *m/z* 477.9 [Ru(*p*-cymene)Cl_2pta-Me]$^+$. Anal. Calcd for $C_{17}H_{29}Cl_3N_3RuP\cdot0.5H_2O$: C, 39.1; H, 5.8; N, 8.0. Found: C, 38.9; H, 5.8; N, 8.1.

Synthesis of [Os(η^6-*p*-cymene)Cl_2pta] (3). A mixture of [Os(η^6-*p*-cymene)Cl_2]$_2$ (100 mg, 0.126 mmol) and pta (39.7 mg, 0.252 mmol) was refluxed under nitrogen in MeOH (25 mL) for 4 h. After evaporation of the solvent under vacuum the residue was washed with ether (2 × 5 mL) and recrystallized from hot methanol. The product was obtained as orange crystals; yield 118.5 mg, 85%. ^{1}H NMR (MeOD-d_4, 400 MHz): δ 1.28 (d, 7.33 Hz, ArCH(CH_3)$_2$), 2.18 (s, ArCH_3), 2.67 (m, ArCH(CH$_3$)$_2$), 4.27 (s, PCH_2N), 4.55 and 4.63 (d, NCH_AH_BN, ^2J = 12.72 Hz). ^{31}P NMR (MeOD-d_4, 162 Hz): δ −80.44. ESI-MS: *m/z* 518.1 [Os(*p*-cymene)Clpta]$^+$. Anal. Calcd for $C_{16}H_{26}Cl_2N_3OsP\cdot0.5H_2O$: C, 34.2; H, 4.8; N, 7.5. Found: C, 34.0; H, 4.7; N, 7.2.

Synthesis of [Os(η^6-*p*-cymene)Cl_2pta-Me]Cl (4). A mixture of [Os(η^6-*p*-cymene)Cl_2] (100 mg, 0.126 mmol) and [pta-Me]Cl (52.3 mg, 0.252 mmol) was refluxed under nitrogen in MeOH (25 mL) for 4 h. After evaporation of the solvent under vacuum the residue was washed with ether (2 × 5 mL) and recrystallized from hot methanol. The product was obtained as orange crystals; yield 104.2 mg, 68% ^{1}H NMR (MeOD-d_4, 400 MHz): δ 1.26 (d, 7 Hz, ArCH(CH_3)$_2$), 2.19 (s, ArCH_3), 2.66 (heptet, 7 Hz, ArCH(CH$_3$)$_2$), 2.84 (d, 2 Hz, N$^+$CH$_3$), 4.21 and 4.33 (d, 15 Hz, PCH_AH_BN), 4.56 (d, 3 Hz, PCH_2N$^+$), 4.49 and 4.62 (d, 14 Hz, NCH_AH_BN), 4.96 and 5.07 (d, 12 Hz, NCH_AH_BN$^+$). ^{31}P NMR (MeOD-d_4, 162 Hz): δ −63.7. ESI-MS: *m/z*

(30) Dyson, P. J.; Ellis, D. J.; Laurenczy, G. *Adv. Synth. Catal.* **2003**, *345*, 211. Gould, R. O.; Jones, C. L.; Robertson, D. R.; Tocher, D. A.; Stephenson, T. A. *J. Organomet. Chem.* **1982**, *226*, 199. Horvath, H.; Laurenczy, G.; Katho, A. *J. Organomet. Chem.* **2004**, *689*, 1036.

(31) Eisen, M. S.; Haskel, A.; Chen, H.; Olmstead, M. M.; Smith, D. P.; Maestre, M. F.; Fish, R. H. *Organometallics* **1995**, *14*, 2806. Kuo, L. Y.; Kanatzidis, M. G.; Sabat, M.; Tipton, A. L.; Marks, T. J. *J. Am. Chem. Soc.* **1991,** *113*, 9027. Smith, D. P.; Baralt, E.; Morales, B.; Olmstead, M. M.; Maestre, M. F.; Fish, R. H. *J. Am. Chem. Soc.* **1992**, *114*, 10647. Smith, D. P.; Griffin, M. T.; Olmstead, M. M.; Maestre, M. F.; Fish, R. H. *Inorg. Chem.* **1993**, *32*, 4677. Smith, D. P.; Kohen, E.; Maestre, M. F.; Fish, R. H. *Inorg. Chem.* **1993**, *32*, 4119. Smith, D. P.; Olmstead, M. M.; Noll, B. C.; Maestre, M. F.; Fish, R. H. *Organometallics* **1993**, *12*, 593.

(32) Akbayeva, D. N.; Gonsalvi, L.; Oberhauser, W.; Peruzzini, M.; Vizza, F.; Bruggeller, P.; Romerosa, A.; Sava, G.; Bergamo, A. *Chem. Commun.* **2003**, 264.

(33) Korn, S.; Sheldrick, W. S. *J. Chem. Soc., Dalton Trans.* **1997**, 2191.

(34) Bennett, M. A.; Smith, A. K. *J. Chem. Soc., Dalton Trans.* **1974**, 233.

(35) Cabeza, J. A.; Maitlis, P. M. *J. Chem. Soc., Dalton Trans.* **1985**, 573. Werner, H.; Zenkert, K. *J. Organomet. Chem.* **1988**, *345*, 151.

(36) Daigle, D. J.; Pepperman, A. B., Jr. *J. Heterocycl. Chem.* **1975**, *12*, 579. Daigle, D. J.; Pepperman, A. B., Jr.; Boudreaux, G. *J. Heterocycl. Chem.* **1974**, *11*, 1085.

(37) Dyson, P. J.; McIndoe, J. S. *Inorg. Chim. Acta* **2003**, *354*, 68.

567.9 [Os(*p*-cymene)Cl_2pta-Me]$^+$. Anal. Calcd for $C_{17}H_{29}Cl_3N_3OsP\cdot 0.5H_2O$: C, 33.4; H, 4.9; N, 6.9. Found: C, 33.6; H, 5.2; N, 6.7.

Crystallography. Data collection was performed at 140(2) K on a mar345 IPDS instrument for **3** and on a four-circle goniometer having κ geometry and equipped with an Oxford Diffraction KM4 Sapphire CCD in the case of compounds **2** and **4**. Data reduction was carried out on all data collections with CrysAlis RED, release 1.7.0.[38] Absorption corrections have been applied to all data sets. Structure solution and refinement as well as molecular graphics and geometrical calculations were performed with the SHELXTL software package, release 5.1.[39] The structures were refined using full-matrix least squares on F^2 with all non-H atoms anisotropically defined. H atoms were placed in calculated positions using the "riding model". Some restraints have been applied, in the case of compounds **2** and **4**, in the refinement of the displacement parameters of the solvent molecule (1/2 CH_3OH).

Oligonucleotide Binding. The 14-mer oligonucleotide 5′-ATACATGGTACATA-3′ was obtained from MWG biotech AG (Ebersberg, Germany), and the concentration was taken to be 187 pmol/μL, as specified by the supplier. The samples were prepared by mixing the 14-mer (2 nmol, 10.7 μL) with an aqueous solution of the complex (1 mg mL^{-1}) with the appropriate stoichiometry (2, 4, or 10 nmol) and completed to 25 μL with pure water. The samples were maintained at 37 °C for 72 h. Experiments conducted at different pHs were performed in phosphate buffer solution at pH 5.8−8. The ESI-MS measurements were performed on a Micromass Q-Tof Ultima. The samples (5 μL) were desalted at 20 °C by HPLC on a C18 Xterra (Waters, Milford) with an acetonitrile gradient from 0 to 30% in 10 min and to 100% of acetonitrile in 5 min; the flow rate was 10 μL/min. Directly after the column, the samples were diluted in two volumes of acetonitrile and injected in the mass spectrometer. The spectra were recorded in negative mode, and before every series of measurements the spectrometer was calibrated with H_3PO_4. The source temperature was set at 373 K and the cone voltage to 35 kV, with a mass range from *m/z* 400 to 2000. The acquisition and deconvolution of data were performed on a Mass Lynx (version 4.0) Windows XP PC system using the Max Ent Electrospray software algorithm.

Computational Methods. All calculations were carried out using density functional theory as implemented in the Gaussian03 package,[40] except where stated otherwise. After initial tests with the BP86,[41,42] BLYP,[41,43] and B3LYP[41,44] exchange-correlation energy functionals, the last functional was used exclusively. According to these initial calculations all investigated compounds can be treated as closed-shell systems (Table S5a−c; Supporting Information). Three different basis sets were employed. Basis 1 is the LanL2DZ basis, which consists of the D95V basis[45] for hydrogen, carbon, nitrogen, and oxygen and the Los Alamos National Laboratories effective semi-core potentials (ECP) (relativistic for Ru and Os) in combination with a double-ζ basis (LanL2DZ) for phosphorus, chlorine,[461] ruthenium, and osmium.[46,47] Basis 2 is a mixed basis set using LanL2DZ for ruthenium or osmium and 6-31+G(d) on the remaining atoms. Basis 3 is a mixed basis set using the quasirelativistic Stuttgart/Dresden semi-core SDD-ECP[48] with a (8s7p6d)/[6s5p3d]-GTO triple-ζ valence basis set on the ruthenium or osmium atoms and 6-31+G(d) on the remaining atoms.

The arene−nucleobase exchange calculations and additional extensive reference calculations were carried out with the ADF 2004.01 package at the generalized gradient approximation (GGA) level of theory.[49] The BP86 and BLYP exchange-correlation energy functionals and the "TZP" basis set of the ADF package were used. This last basis set is of triple-ζ quality with one polarization function in the valence region and a double-ζ representation in the core region. The frozen-core approximation (for electrons up to the 1s shell for C, N, and O, up to 2p for P and Cl, 3d for Ru, and 4d for Os) and a spin-restricted formalism were applied. The ZORA approach was used to incorporate scalar relativistic effects.[50]

The CPMD[51] program was used for reference calculations on the ruthenium compounds. An analytical local pseudopotential (PP) for hydrogen atoms and nonlocal, norm-conserving soft PPs of the Martins−Trouiller[52] type for all other elements were used. The same valence electrons as with ADF have been treated explicitly and the PP for ruthenium incorporates scalar relativistic effects. The PPs for C, N, P, and Cl were transformed to a fully nonlocal form using the scheme of Kleinman and Bylander,[53] whereas for Ru the semi-core PP was integrated numerically using a Gauss−Hermite quadrature. The BP86 and BLYP exchange-correlation energy functionals were used.

Geometries and wave functions were optimized by starting from the crystal structure of **1** or modifications thereof using basis 1. Proper convergence was, whenever necessary, verified via frequency analysis.

The results were further refined using basis 2 and basis 3. The same procedure was applied to the crystal structure of **7**. Reference calculations with different functionals and basis sets were carried out by starting with these structures (see the Supporting Information). The basis set superposition error (BSSE) was calculated with basis 2 and basis 3 for compounds **1**−**7** (Tables S1a and S2a). Basis 3 agrees best with the CPMD

(38) *CrysAlis RED*, 1.7.0; Oxford Diffraction Ltd., Abingdon, Oxfordshire, U.K., 2003.
(39) Sheldrick, G. M. *SHELXTL*, Version 6.10; Bruker AXS Inc., Madison, WI, 2000. Sheldrick, G. M. *SHELXS97* and *SHELXL97*; University of Göttingen, Göttingen, Germany, 1997.
(40) Frisch, M. J.; Trucks, G. W.; Schlegel, H. B.; Scuseria, G. E.; Robb, M. A.; Cheeseman, J. R.; Montgomery, J. A., Jr.; Vreven, T.; Kudin, K. N.; Burant, J. C.; Millam, J. M.; Iyengar, S. S.; Tomasi, J.; Barone, V.; Mennucci, B.; Cossi, M.; Scalmani, G.; Rega, N.; Petersson, G. A.; Nakatsuji, H.; Hada, M.; Ehara, M.; Toyota, K.; Fukuda, R.; Hasegawa, J.; Ishida, M.; Nakajima, T.; Honda, Y.; Kitao, O.; Nakai, H.; Klene, M.; Li, X.; Knox, J. E.; Hratchian, H. P.; Cross, J. B.; Adamo, C.; Jaramillo, J.; Gomperts, R.; Stratmann, R. E.; Yazyev, O.; Austin, A. J.; Cammi, R.; Pomelli, C.; Ochterski, J. W.; Ayala, P. Y.; Morokuma, K.; Voth, G. A.; Salvador, P.; Dannenberg, J. J.; Zakrzewski, V. G.; Dapprich, S.; Daniels, A. D.; Strain, M. C.; Farkas, O.; Malick, D. K.; Rabuck, A. D.; Raghavachari, K.; Foresman, J. B.; Ortiz, J. V.; Cui, Q.; Baboul, A. G.; Clifford, S.; Cioslowski, J.; Stefanov, B. B.; Liu, G.; Liashenko, A.; Piskorz, P.; Komaromi, I.; Martin, R. L.; Fox, D. J.; Keith, T.; Al-Laham, M. A.; Peng, C. Y.; Nanayakkara, A.; Challacombe, M.; Gill, P. M. W.; Johnson, B.; Chen, W.; Wong, M. W.; Gonzalez, C.; Pople, J. A. *Gaussian 03*, revision B.03; Gaussian, Inc.: Pittsburgh, PA, 2003.
(41) Becke, A. D. *J. Chem. Phys.* **1993**, *98*, 5648.
(42) Perdew, J. P. *Phys. Rev. B: Condens. Matter Mater. Phys.* **1986**, *33*, 8822.
(43) Lee, C.; Yang, W.; Parr, R. G. *Phys. Rev. B: Condens. Matter Mater. Phys.* **1988**, *37*, 785.
(44) Becke, A. D. *Phys. Rev. A: At., Mol., Opt. Phys.* **1988**, *38*, 3098.
(45) Dunnung, T. H., Jr., Hay, P. J., Eds. Plenum: New York, 1976; Vol. 3, p 1.
(46) Wadt, W. R.; Hay, P. J. *J. Chem. Phys.* **1985**, *82*, 284.
(47) Hay, P. J.; Wadt, W. R. *J. Chem. Phys.* **1985**, *82*, 270. Hay, P. J.; Wadt, W. R. *J. Chem. Phys.* **1985**, *82*, 299.
(48) Andrae, D.; Haeussermann, U.; Dolg, M.; Stoll, H.; Preuss, H. *Theor. Chim. Acta* **1990**, *77*, 123.
(49) *ADF2004.01*; SCM, Vrije Universiteit, Amsterdam, The Netherlands, 2004. Guerra, C. F.; Snijders, J. G.; te Velde, G.; Baerends, E. J. *Theor. Chem. Acc.* **1998**, *99*, 391; te Velde, G.; Bickelhaupt, F. M.; Baerends, E. J.; Fonseca Guerra, C.; Van Gisbergen, S. J. A.; Snijders, J. G.; Ziegler, T. *J. Comput. Chem.* **2001**, *22*, 931.
(50) van Lenthe, E.; Baerends, E. J.; Snijders, J. G. *J. Chem. Phys.* **1994**, *101*, 9783. van Lenthe, E.; Baerends, E. J.; Snijders, J. G. *J. Chem. Phys.* **1993**, *99*, 4597. van Lenthe, E.; Ehlers, A.; Baerends, E.-J. *J. Chem. Phys.* **1999**, *110*, 8943.
(51) Hutter, J.; Ballone, P.; Bernasconi, M.; Focher, P.; Fois, E.; Goedecker, S.; Parrinello, M.; Tuckerman, M. *CPMD*; Max-Planck Institut für Festkörperforschung, Stuttgart, Germany, and IBM Research Laboratory, Zürich, Switzerland, 1998.
(52) Troullier, N.; Martins, J. L. *Phys. Rev. B: Condens. Matter Mater. Phys.* **1991**, *43*, 1993.
(53) Kleinman, L.; Bylander, D. M. *Phys. Rev. Lett.* **1982**, *48*, 1425.

results, which are per definition BSSE-free. Calculations on the osmium compounds were performed by starting from the optimized ruthenium structures, as the crystal structures of **2**−**4** were not yet available. However, reference calculations starting from the crystal structure of **3** yielded identical geometries and energies.

The reported BEs were calculated using the general formulas

$$E_{\text{binding}} = E(\text{MXCl}_n) + E(\text{Y}) - E(\text{MXYCl}_n)$$

$$E_{\text{binding}} = E(\text{MYCl}_n) + E(\text{X}) - E(\text{MXYCl}_n)$$

where M = Ru, Os, X = PTA, *N*-methyl-PTA$^+$, *N*-protonated-PTA$^+$, dien, Y = arene, and n = number of chloride anions in the complex.

Reference calculations for the reaction M^0(Ru,Os)(g) + $2C_5H_5$(radical)(g) → $M(C_5H_5)_2$(g) for which calorimetric energies are available show the B3LYP functional to provide better binding energies than the BP86 functional (Table S8).

The absolute magnitudes of the metal−arene interactions are found to be very sensitive to the method (functional and basis set type) applied. However, the trends are essentially the same for all methods used. We observed nearly constant shifts for different types of basis sets (Gaussian type, Slater type, plane waves) as well as for different correlation parts of the functional (LYP, 3LYP, P86). Basis 2 and basis 3 yield the same binding energies for all investigated osmium compounds, but in the case of the ruthenium−arene interactions, basis 3 results in a further stabilization of about 5 kcal/mol compared to basis 2. Reference calculations with ADF and CPMD show that this difference is most probably due to the LanL2DZ basis which, although providing good geometries for both ruthenium and osmium compounds, does calculate weaker ruthenium−arene interactions. As was already reported for other ruthenium and osmium complexes, the BP86 functional calculates BEs that are 10−17 kcal/mol higher than their B3LYP analogues (Tables S1a, S1b, and S2a).[24] Again, the relative differences between the complexes (Tables S1c and S2b) are, however, very similar.

As can be concluded from Tables S1a and S3, the use of PH_3 as a replacement for pta changes the metal−arene BE significantly and is therefore not appropriate as a reduced computational model.

To calculate the corresponding η^6 interaction energies of the nucleobases with ruthenium, we placed the aromatic five- and six-membered rings of the nucleobases in the position of the η^6 benzene in compound **5** and screened the potential energy surface for minima by starting geometry optimizations from different initial structures. In the case of cytosine and the six-membered ring of guanine, also a starting structure with explicit ruthenium σ-binding to the N3 atom was investigated.

Acknowledgment. We thank the EPFL and the Swiss National Science Foundation for financial support.

Supporting Information Available: Structural data, ligand binding energies, and spin states calculated with various methods. This material is available free of charge via the Internet at http://pubs.acs.org.

OM049022A